

Dynamical Computing on the Nanoscale: Superconducting Circuits for Thermodynamically-Efficient Classical Information Processing

Christian Z. Pratt,^{*} Kyle J. Ray,[†] and James P. Crutchfield[‡]
Complexity Sciences Center and Department of Physics and Astronomy,
University of California, Davis, One Shields Avenue, Davis, CA 95616
(Dated: September 13, 2023)

Alternative computing paradigms open the door to exploiting recent innovations in computational hardware. Dynamical computing is one such paradigm that synthesizes momentum computing—an extremely energy-efficient design framework—with nanoscale thermodynamic computing. This synthesis can be implemented with Josephson junction technology, giving a testbed with tunable coupling to a thermal environment. Investigating the dynamics and thermodynamics of these superconducting quantum interference devices (SQUIDs), though, requires (i) constructing physically-realizable superconducting circuits, (ii) thoroughly understanding circuit energetics, and (iii) designing sufficiently complex circuits that support a suite of useful operations. First-principle circuit design leads to prohibitive algebraic complications that precluded achieving these goals quickly and efficiently. We circumvent these complications by (i) specializing our class of circuits and regime of operation, (ii) synthesizing existing methods to suit these specializations, and (iii) implementing solution-finding optimizations that facilitate physically interpreting circuit degrees of freedom that respect physically-grounded constraints. Practically, this leads to efficient circuit prototyping and analysis and access to scalable circuit architectures. The analytical efficiency is demonstrated by directly reproducing the thermodynamic potential induced by the variable β rf ($v\beta$ -rf) SQUID. We then show how inductively coupling two $v\beta$ -rf SQUIDs to construct a device capable of performing 2-bit computations. The methods detailed here will provide a basis to construct universal logic gates and investigate their thermodynamic performance.

I. INTRODUCTION

All computation is physical—to effect information processing, a sequence of stochastic transformations systematically manipulates a system’s potential energy landscape [1, 2]. Reliable computing, in particular, requires stable memory states physically supported by a system’s information-bearing degrees of freedom [3]. Energy minima on the landscape provide this dynamical stability. Computation, then, consists of externally controlling the creation, destruction, and location of energy minima. This perspective allows quantitatively comparing the computational capabilities and thermodynamic performance of alternative computing paradigms [4].

Dynamical computing aims to consolidate *momentum computing* [2, 5] and *thermodynamic computing* [3, 6, 7]. The result is a paradigm capable of carrying out highly energy-efficient computations, which can be practically implemented using superconducting circuit nanotechnology.

Exploring a superconducting circuit’s ability to perform computational operations involves understanding the device’s energetics and subsequent dynamical equations of motion [8–12]. The following introduces a method to create physically-realizable dynamical computing devices at the nanoscale. Success in this, though, requires rapidly prototyping devices. And this, in turn, demands a calculational framework that can quickly assess the performance of candidate circuits.

The following synthesizes several previous approaches, specializing them to a class of circuits that are of practical

interest. The result is a superconducting circuit formalism that generates an interpretable circuit Lagrangian and associated equations of motion given in terms of classical information-bearing degrees of freedom. In this, a circuit’s potential energy surface is used to gauge its computational capabilities. The framework’s success is demonstrated through the example of the variable β rf ($v\beta$ -rf) superconducting quantum interference device (SQUID) [8, 9]. Inductively coupling two $v\beta$ -rf SQUIDs produces a device that performs 2-bit computations.

II. RELATED WORK

While our development synthesizes methods in Refs. [13–16], it specializes to a particular class of circuits and investigates the dynamical and thermodynamical behavior of the circuit’s degrees of freedom in the classical domain.

Its methodological foundations build on Refs. [13, 14], which introduced a network-theoretic approach to electrical circuit analysis and investigated circuits operating in the quantum regime. Reference [15] provided an elegant technique for multi-loop circuits to find *irrotational* degrees of freedom. However, it considered only the phase space of a quantum circuit’s Hamiltonian. In this way, it departs from our goals. Moreover, to avoid cyclic coordinates in the equations of motion, Ref. [15] restricted each circuit loop to have only a single inductor. The following, though, eschews this restriction. It instead develops optimal solutions for circuits containing more than one

inductor by eliminating the extra degrees of freedom algebraically.

Here, we use the resistive capacitive shunted junction (RCSJ) model for each Josephson junction (JJ). Due to this, the dissipative dynamics arising from finite-valued DC resistances must be accounted for. To do this, we rely on Ref. [16], which provided a method that uses the Rayleigh dissipation function [17] to analyze a circuit's resistive shunts.

Several alternative approaches are available to analyze circuit behaviors in the quantum regime. One common procedure employs number-phase quantization [18, 19], which does not involve a network-theoretic approach. Simulations of the quantum dynamics of similar circuits are detailed in Ref. [20]. This all noted, though the SQUIDS we employ are often the basis for quantum computing devices, we concentrate on their behavior in the classical nonlinear dynamical regime.

Finally, a complementary approach to circuit analysis considers the charge in a loop, as opposed to flux variables [21]. However, previous and proposed experiments with thermodynamic and momentum computing [4, 5, 8] revealed that tuning external fluxes provides a convenient circuit control method. Consequently, this grounds the following in a flux-focused interpretation of circuit behavior. A generalized approach to the techniques implemented in Ref. [15] considers arbitrary circuit geometries and electromagnetic fields to construct a Hamiltonian [22]. That said, analytical complications that arise in this kind of first-principle method preclude rapidly characterizing candidate circuit designs. In contrast, the following provides a workable alternative.

III. SUPERCONDUCTING CIRCUIT ANALYSIS

First, we obtain the equations of motion for a given circuit. Then, we detail an approach for determining coordinates that produce circuit equations of motion in Langevin form.

A. Circuit Equations of Motion

Following Ref. [13], we define a *branch* to be a particular circuit element, whose time dependent *flux* is defined by:

$$\begin{aligned} \phi_b &= \phi_b(t) \\ &:= \int_{-\infty}^t dt' v_b(t') . \end{aligned}$$

This is related to the branch voltage $v_b(t)$, the instantaneous voltage across the circuit element, and the reduced flux $\varphi_b = 2\pi\phi_b/\phi_0$, where ϕ_0 is the flux quantum.

Before proceeding, several assumptions need to be addressed. To begin, all branches within a circuit correspond to either a Josephson junction (JJ) or an inductor.

Corresponding variables are subscripted with a J or L , respectively. All JJs are described by the RCSJ model [23, 24], which is characterized by a critical current I_c [11], capacitance C_J , and resistance R . Each inductive branch is modeled by an inductance L in parallel with a capacitance C_L satisfying the limit $C_L/C_J \approx 0$. We adopt C_L as an auxiliary variable in a fashion similar to Ref. [15], in that the limit is used at a particular step in the calculations, which is exemplified in Sections IV A and IV B.

Suppose a circuit is constructed with n JJs and m inductors for a total of $N = n + m$ branches. The *branch flux* vector $\Phi_b := (\phi_{J_1}, \dots, \phi_{J_n}, \phi_{L_1}, \dots, \phi_{L_m})^T$ compactly represents all circuit branch fluxes. When computing the potential and equations of motion, we refer to the truncated branch flux vectors $\Phi_{b_J} := (\phi_{J_1}, \dots, \phi_{J_n})^T$ and $\Phi_{b_L} := (\phi_{L_1}, \dots, \phi_{L_m})^T$.

The energy stored in the capacitive components is [13]:

$$\mathcal{L}_T = \frac{1}{2} \dot{\Phi}_b^T \mathbf{C} \dot{\Phi}_b , \quad (1)$$

where the *capacitance* matrix is

$$\mathbf{C} := \text{diag} (C_{J_1}, \dots, C_{J_n}, C_{L_1}, \dots, C_{L_m}) .$$

Since we assume that all branches are *either* inductors or JJs, the energy stored in the inductive elements can be calculated using only Φ_{b_L} . The $m \times m$ *inductance* matrix \mathbf{L} denotes the circuit's linear inductances, with diagonal entries corresponding to self-inductances L_i and off-diagonal entries corresponding to the mutual inductive coupling $-M_{ij}$ between L_i and $L_{j \neq i}$. The energy stored in these components [13] is given by:

$$\mathcal{L}_L = \frac{1}{2} \Phi_{b_L}^T \mathbf{L}^{-1} \Phi_{b_L} . \quad (2)$$

Up to a constant, the JJ potential energy contribution [13] is

$$\mathcal{L}_J = - \sum_{i=1}^n E_i \cos \left(\frac{2\pi}{\phi_0} \Phi_{b_J i} \right) , \quad (3)$$

where $E_i = (\phi_0/2\pi)I_c$ is the Josephson energy of the i th JJ in a circuit.

Equations (2) and (3) together give the circuit's conservative potential energy $\mathcal{L}_V := \mathcal{L}_J + \mathcal{L}_L$. Given a physical circuit consisting of inductors and JJs as described above, the circuit Lagrangian $\mathcal{L} := \mathcal{L}_T - \mathcal{L}_V$ is, up to a constant:

$$\begin{aligned} \mathcal{L} &= \frac{1}{2} \dot{\Phi}_b^T \mathbf{C} \dot{\Phi}_b - \frac{1}{2} \Phi_{b_L}^T \mathbf{L}^{-1} \Phi_{b_L} \\ &\quad + \sum_{i=1}^n E_i \cos \left(\frac{2\pi}{\phi_0} \Phi_{b_J i} \right) . \end{aligned} \quad (4)$$

The nonconservative dissipation from the finite JJ resistive shunts are taken into account by the Rayleigh dissipation function \mathcal{D} , and further incorporated into the

Euler-Lagrange equations of motion [16, 17], in terms of generalized coordinate q_i , as:

$$\frac{d}{dt} \frac{\partial \mathcal{L}}{\partial \dot{q}_i} - \frac{\partial \mathcal{L}}{\partial q_i} = - \frac{\partial \mathcal{D}}{\partial \dot{q}_i} , \quad (5)$$

with

$$\mathcal{D} := \sum_{i=1}^n \frac{1}{2R_i} (\dot{\phi}_{J_i})^2 . \quad (6)$$

\mathcal{D} accounts for the dissipated power in each JJ branch due to its shunt resistance R_i in terms of its branch flux ϕ_{J_i} . Recalling that only JJ branches have DC resistance values, we rewrite Eq. (6) as:

$$\mathcal{D} = \frac{1}{2} \dot{\mathbf{\Phi}}_{\text{bJ}}^T \mathbf{D}^{-1} \dot{\mathbf{\Phi}}_{\text{bJ}} ,$$

whereby, following the same logic as with \mathbf{L}^{-1} , \mathbf{D} has dimensions of $n \times n$. However, unlike \mathbf{L} , \mathbf{D} is manifestly diagonal.

To conclude, we add the contribution of the DC resistances' thermal noise current to the equations of motion via:

$$\frac{d}{dt} \frac{\partial \mathcal{L}}{\partial \dot{q}_i} - \frac{\partial \mathcal{L}}{\partial q_i} = - \frac{\partial \mathcal{D}}{\partial \dot{q}_i} + \eta_i(t) , \quad (7)$$

in which $\eta_i(t)$ is nonzero for the JJ branches only. As is standard in Langevin treatments [25], $\eta_i(t)$ are statistically independent of each other and delta correlated over time, in conjunction with their magnitudes being determined by the fluctuation-dissipation theorem through the relation:

$$\langle \eta_i(t) \eta_i(t') \rangle = \frac{2k_B T}{R_i} \delta(t - t') .$$

B. Determining Optimal Coordinates

Despite the fact that Eq. (5) marginally accommodates the circuit's topology, it does not account for fluxoid quantization conditions [13, 26]. These require that the sum of the branch fluxes around any loop equals the external flux threading the loop. As a result, while there may appear to be $N = n + m$ degrees of freedom in the Lagrangian, there are only $N - F$ degrees of freedom in a circuit with F independent loops—i.e., loops that contain no other loops—threaded by external fluxes.

In view of this, the *external flux* vector $\mathbf{\Phi}_x := (\phi_{x_1}, \dots, \phi_{x_F})^T$ is defined to cast fluxoid quantization in matrix form [15]:

$$\mathbf{\Phi}_x = \mathbf{R} \mathbf{\Phi}_b .$$

The $F \times N$ matrix \mathbf{R} is constructed in such a way that its elements R_{ij} satisfy the following criteria: Let \mathbf{L}_i denote

the i th loop threaded by the external flux Φ_{x_i} that may contain branch flux ϕ_j , then:

$$R_{ij} := \begin{cases} +1 & \phi_j \in \mathbf{L}_i \text{ same orientation as } \Phi_{x_i} , \\ -1 & \phi_j \in \mathbf{L}_i \text{ opposite orientation as } \Phi_{x_i} , \text{ and} \\ 0 & \phi_j \notin \mathbf{L}_i . \end{cases}$$

Finally, the circuit's degrees of freedom are defined as $\tilde{\mathbf{\Phi}} := (\tilde{\phi}_1, \dots, \tilde{\phi}_{N-F})^T$. Generally, these are a to-be-determined linear combination of the branch fluxes represented by the $(N - F) \times N$ matrix \mathbf{M} :

$$\tilde{\mathbf{\Phi}} = \mathbf{M} \mathbf{\Phi}_b .$$

Furthermore, due to fluxoid quantization, no more than $N - F$ degrees of freedom in the circuit are expected. The quantization conditions are included by employing the $N \times 1$ *augmented* vector $\tilde{\mathbf{\Phi}}_+$ and the $N \times N$ *augmented* matrix \mathbf{M}_+ :

$$\tilde{\mathbf{\Phi}}_+ := \begin{pmatrix} \tilde{\mathbf{\Phi}} \\ \mathbf{\Phi}_x \end{pmatrix} ,$$

$$\mathbf{M}_+ := \begin{pmatrix} \mathbf{M} \\ \mathbf{R} \end{pmatrix} .$$

Note that the branch flux vector and the augmented flux vector are directly related to each other through \mathbf{M}_+ by:

$$\tilde{\mathbf{\Phi}}_+ = \mathbf{M}_+ \mathbf{\Phi}_b . \quad (8)$$

With this, the circuit Lagrangian and associated equations of motion can be written in terms of $\tilde{\mathbf{\Phi}}$ by substituting $\mathbf{\Phi}_b = \mathbf{M}_+^{-1} \tilde{\mathbf{\Phi}}_+$ into Eq. (5). Specifically, to find the circuit's Lagrangian in terms of $\tilde{\mathbf{\Phi}}$, \mathbf{M}_+ must be invertible. Provided that the columns of \mathbf{M} are chosen to be linearly independent of each other and of the columns of \mathbf{R} , nonsingularity of \mathbf{M}_+ is guaranteed.

However, ambiguity remains in defining \mathbf{M} 's elements. Following Ref. [15], the degrees of freedom are deemed *irrotational* by ensuring they satisfy the following constraint:

$$\mathbf{R} \mathbf{C}^{-1} \mathbf{M}^T = \mathbf{0} . \quad (9)$$

This guarantees that the Lagrangian, when written in terms of $\tilde{\mathbf{\Phi}}$, does not depend on $\mathbf{\Phi}_x$. Due to this, $\tilde{\mathbf{\Phi}}$ is referred to as the *irrotational flux* vector. In addition, Eq. (9) allows the equations of motion to be of Langevin form, further enabling thermodynamical analyses of the circuit's information-bearing degrees of freedom.

However, even after enforcing the irrotational constraint, there is still additional freedom in defining \mathbf{M} . To address this, we turn to the kinetic energy term:

$$\mathcal{L}_T = \frac{1}{2} \dot{\mathbf{\Phi}}_b^T \mathbf{C} \dot{\mathbf{\Phi}}_b \quad (10)$$

$$= \frac{1}{2} \dot{\mathbf{\Phi}}_+^T (\mathbf{M}_+^{-1})^T \mathbf{C} \mathbf{M}_+^{-1} \dot{\mathbf{\Phi}}_+ \\ = \frac{1}{2} \dot{\mathbf{\Phi}}_+^T \mathbf{C}_{\text{eff}} \dot{\mathbf{\Phi}}_+ . \quad (11)$$

With Eq. (11) in mind, recall that the goal is to obtain an easily interpretable Lagrangian and corresponding equations of motion for a given circuit. A diagonal \mathbf{C}_{eff} allows for a straightforward interpretation of \mathcal{L}_T as the kinetic energy of the Lagrangian in both the Φ_b and the $\tilde{\Phi}$ bases. In other words, the task is to find solutions of \mathbf{M} that yield a diagonal \mathbf{C}_{eff} .

Analyzing a number of cases established a set of calculational guidelines that result in a diagonal \mathbf{C}_{eff} when solving for the components of \mathbf{M} through Eq. (9). These aid in the task of finding optimal solutions in the continuous family of possible solutions:

1. The first n rows of \mathbf{M} can each contain up to n nonzero entries corresponding to the n JJ coefficients of $\mathbf{M}\Phi_b$, which will have the same magnitude. The other m inductive elements of \mathbf{M} , corresponding to the inductive coefficients in each of these rows, will either be zero or proportional to C_L/C_J ; the latter subsequently vanishes when $C_L/C_J \rightarrow 0$. Note that this limit is taken after a solution is found.
2. The last $|m - F|$ rows of \mathbf{M} will each contain up to m nonzero entries corresponding to the m inductive flux coefficients of $\mathbf{M}\Phi_b$, which also have the same magnitude. All n JJ coefficients in each row will contain zero entries, and all nonzero inductive coefficients are unity herein.

Importantly, linear independence between rows must be maintained when implementing these conditions.

To briefly illustrate guideline (1), one possible realization is that in each of the n rows, every JJ coefficient takes on a nonzero value only once, while all other JJ coefficients are zero. If each nonzero value is unity, this is equivalent to there being no coordinate space rotation between branch and irrotational flux coordinates.

Guideline (2) stems from a mismatch between the number of loops and inductors. For example, setting $|m - F| = 1$ —i.e., there is one loop that contains more than one inductor—requires setting all JJ coefficients to zero for one solution of Eq. (9). This reflects the inability of an irrotational degree of freedom to describe the additional inductor's behavior in the circuit. Consequently, one cyclic coordinate appears in the circuit Lagrangian; this can be eliminated through determining its equation of motion and subsequently rewriting it in terms of non-cyclic irrotational degrees of freedom. Sections IV A and IV B below demonstrate this procedure.

Once the elements of \mathbf{M} are determined, the number of *dynamical* degrees of freedom are interpreted as the irrotational degrees of freedom that are not cyclic [17]. Numerically, there are $N - F - |m - F|$, as there will be $N - F$ irrotational flux coordinates with $|m - F|$ expected to be cyclic. For a multi-loop circuit ($F > 1$), a diagonal \mathbf{C}_{eff} is found only when there are no more JJs than there are irrotational degrees of freedom. Equivalently, the number of inductors in a circuit containing both JJs

and inductors must be greater than or equal to F ; i.e., $m \geq F$. These conditions can also be explained as the following: Each JJ must be physically represented by at least one dynamical degree of freedom, and there must be at least one inductor per independent circuit loop to capture the circuit flux behavior. Below, we illustrate these conditions by example.

IV. EXAMPLE DEVICE DESIGNS

The following demonstrates the circuit design method via two examples: A variable β rf SQUID and a circuit that implements 2-bit computations.

A. Variable β rf SQUID

Consider analyzing the $v\beta$ -rf SQUID implemented by Ref. [9] and shown in Fig. 1. One motivation is to reproduce the two-dimensional potential created by the circuit via the introduced formalism. Notably, though, the result shows that the methodology is not only useful and computationally efficient, but also reproduces the results of previous approaches.

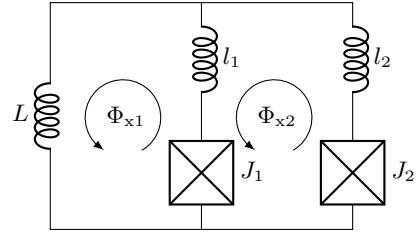


FIG. 1. A $v\beta$ -rf SQUID with $N = 5$ and $F = 2$. Slight adjustments are made to the physical construction of the circuit to compare to Ref. [9].

As such, the circuit analysis boils down to finding a coordinate transformation that leaves the equations of motion in the form of Langevin dynamics in terms of dynamical degrees of freedom. Note that:

$$\begin{aligned}\Phi_b &= (\phi_{J_1} \ \phi_{J_2} \ \phi_L \ \phi_{l_1} \ \phi_{l_2})^T, \\ \Phi_{b_J} &= (\phi_{J_1} \ \phi_{J_2})^T, \\ \Phi_{b_L} &= (\phi_L \ \phi_{l_1} \ \phi_{l_2})^T, \\ \tilde{\Phi}_+ &= (\tilde{\phi}_1 \ \tilde{\phi}_2 \ \tilde{\phi}_3 \ \phi_{x_1} \ \phi_{x_2})^T.\end{aligned}$$

With every branch orientation in Fig. 1 pointing upwards, fluxoid quantization gives:

$$\mathbf{R} = \begin{pmatrix} 1 & 0 & -1 & 1 & 0 \\ -1 & 1 & 0 & -1 & 1 \end{pmatrix},$$

where each row's entries correspond to the column orientation of $\{J_1, J_2, L, l_1, l_2\}$, respectively. This suggests

that

$$\mathbf{C}^{-1} = \text{diag}(C_{J_1}^{-1}, C_{J_2}^{-1}, C_L^{-1}, C_{l_1}^{-1}, C_{l_2}^{-1}).$$

To satisfy Eq. (9), let:

$$\mathbf{M}^\top = \begin{pmatrix} M_{11} & M_{21} & M_{31} \\ M_{12} & M_{22} & M_{32} \\ M_{13} & M_{23} & M_{33} \\ M_{14} & M_{24} & M_{34} \\ M_{15} & M_{25} & M_{35} \end{pmatrix}.$$

Then, with the assumption that $C_l := C_{l_1} = C_{l_2} = C_L$ and $C_J := C_{J_1} = C_{J_2}$, each column of \mathbf{M}^\top satisfies:

$$CM_{i1} = M_{i3} - M_{i4} \quad (12)$$

$$C(M_{i2} - M_{i1}) = M_{i4} - M_{i5},$$

with $C := C_l/C_J$ and $i = 1, 2, 3$. To implement guideline (1) for the first $n = 2$ rows of \mathbf{M} and guideline (2) for the last $|m - F| = 1$ row of \mathbf{M} , we write a subset of the solution space of Eq. (12) in the augmented matrix:

$$\mathbf{M}_+ = \begin{pmatrix} \mathbf{M} \\ \mathbf{R} \end{pmatrix} = \begin{pmatrix} 1/2 & 1/2 & C/4 & -C/4 & -C/4 \\ -1 & 1 & 0 & C & -C \\ 0 & 0 & 1 & 1 & 1 \\ 1 & 0 & -1 & 1 & 0 \\ -1 & 1 & 0 & -1 & 1 \end{pmatrix}. \quad (13)$$

Guidelines (1) and (2) are realized by taking $C \rightarrow 0$. Consequently, we expect there to be $|m - F| = 1$ cyclic irrotational degree of freedom once the circuit Lagrangian \mathcal{L} is found.

Next, inverting \mathbf{M}_+ yields:

$$\mathbf{M}_+^{-1} = \begin{pmatrix} 1 & -1/2 & 0 & 0 & 0 \\ 1 & 1/2 & 0 & 0 & 0 \\ 2/3 & 0 & 1/3 & -2/3 & -1/3 \\ -1/3 & 1/2 & 1/3 & 1/3 & -1/3 \\ -1/3 & -1/2 & 1/3 & 1/3 & 2/3 \end{pmatrix}, \quad (14)$$

which, through Eq. (11), aids in computing:

$$\mathbf{C}_{\text{eff}} = \begin{pmatrix} 2C_J & 0 & 0 & 0 & 0 \\ 0 & C_J/2 & 0 & 0 & 0 \\ 0 & 0 & 0 & 0 & 0 \\ 0 & 0 & 0 & 0 & 0 \\ 0 & 0 & 0 & 0 & 0 \end{pmatrix}$$

in the expected form.

As there are no mutual inductance couplings, the inductance matrix is:

$$\mathbf{L} = \begin{pmatrix} L & 0 & 0 \\ 0 & l_1 & 0 \\ 0 & 0 & l_2 \end{pmatrix}.$$

Recalling Eq. (8) and writing the circuit Lagrangian from Eq. (4) in terms of irrotational branch fluxes, produces:

$$\begin{aligned} \mathcal{L} = & \frac{C_J}{2} \left(2\dot{\tilde{\phi}}_1^2 + \frac{1}{2}\dot{\tilde{\phi}}_2^2 \right) \\ & - \frac{1}{9L} \left(2\tilde{\phi}_1 + \tilde{\phi}_3 - 2\phi_{x_1} - \phi_{x_2} \right)^2 \\ & - \frac{1}{9l_1} \left(-\tilde{\phi}_1 + \frac{3}{2}\tilde{\phi}_2 + \tilde{\phi}_3 + \phi_{x_1} - \phi_{x_2} \right)^2 \\ & - \frac{1}{9l_2} \left(-\tilde{\phi}_1 - \frac{3}{2}\tilde{\phi}_2 + \tilde{\phi}_3 + \phi_{x_1} + 2\phi_{x_2} \right)^2 \\ & + E_{2+1} \cos \tilde{\varphi}_1 \cos \frac{\tilde{\varphi}_2}{2} - E_{2-1} \sin \tilde{\varphi}_1 \sin \frac{\tilde{\varphi}_2}{2}, \end{aligned} \quad (15)$$

where $E_{2\pm 1} = E_{J_2} \pm E_{J_1}$.

The Lagrangian is independent of $\dot{\tilde{\phi}}_3$ which indicates that it is, as expected, a cyclic degree of freedom; it can be eliminated by computing its equation of motion, finding that $\tilde{\phi}_3 = \tilde{\phi}_1 - \phi_{x_1} - \phi_{x_2}/2$, and substituting this into \mathcal{L} . We can now identify a map between the irrotational flux variables and the fluxes appearing in Ref. [9]:

$$\begin{aligned} \tilde{\phi}_1 &= \phi, \\ \tilde{\phi}_2 &= \phi_{\text{dc}}, \\ \phi_{x_1} &= \phi_x - \frac{1}{2}\phi_{\text{xdc}}, \text{ and} \\ \phi_{x_2} &= \phi_{\text{xdc}}. \end{aligned}$$

Making these substitutions into Eq. (15) yields a Lagrangian \mathcal{L} that matches that of Ref. [9] with the preceding variable substitutions:

$$\begin{aligned} \mathcal{L} &= \mathcal{L}_T - \mathcal{L}_{v\beta\text{-rf}} \\ &= \frac{C_J}{2} \left(2\dot{\phi}^2 + \frac{1}{2}\dot{\phi}_{\text{dc}}^2 \right) \\ &\quad - \frac{1}{2L} (\phi - \phi_x)^2 - \frac{1}{2l} (\phi_{\text{dc}} - \phi_{\text{xdc}})^2 \\ &\quad + E_{2+1} \cos \varphi \cos \frac{\varphi_{\text{dc}}}{2} - E_{2-1} \sin \varphi \sin \frac{\varphi_{\text{dc}}}{2}. \end{aligned} \quad (16)$$

B. Inductively Coupled $v\beta$ -rf SQUIDs

Consider inductively coupling two $v\beta$ -rf SQUIDs through L_1 and L_2 via the mutual inductance $M := M_{12} = M_{21}$, shown in Fig. 2. This device enables 2-bit classical computations, which is physically realized by controlling the adjustable circuit parameters ϕ_{ix} and $\phi_{ix\text{dc}}$ for $i = 1, 2$, as well as M . While we consider M to be a tunable constant herein, the details of the coupler's physical construction, such as those detailed in Refs. [27–29], will be addressed elsewhere. Now, let's derive the potential.

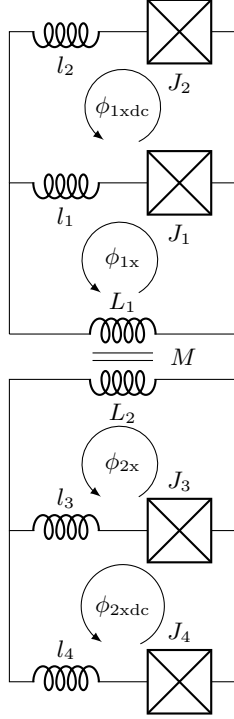


FIG. 2. Two $v\beta$ -rf SQUIDs inductively coupled via M : A superconducting device that supports 2-bit classical computations.

The choice of flux quantization is represented in circuit network-theoretic terms through:

$$\mathbf{R} = \begin{pmatrix} 1 & 0 & 0 & 0 & -1 & 0 & 1 & 0 & 0 & 0 \\ -1 & 1 & 0 & 0 & 0 & 0 & -1 & 1 & 0 & 0 \\ 0 & 0 & 1 & 0 & 0 & -1 & 0 & 0 & 1 & 0 \\ 0 & 0 & -1 & 1 & 0 & 0 & 0 & 0 & -1 & 1 \end{pmatrix}.$$

Using the irrotational constraint $\mathbf{R}\mathbf{C}^{-1}\mathbf{M}^T = \mathbf{0}$, we find that the elements of \mathbf{M} need to satisfy:

$$\begin{aligned} CM_{i1} &= M_{i5} - M_{i7} \\ C(M_{i2} - M_{i1}) &= M_{i7} - M_{i8} \\ CM_{i3} &= M_{i6} - M_{i9} \\ C(M_{i4} - M_{i3}) &= M_{i9} - M_{i10}. \end{aligned}$$

Taking a lesson from the single $v\beta$ -rf case and after taking $C \rightarrow 0$, our choice of \mathbf{M} becomes:

$$\mathbf{M}_+ = \begin{pmatrix} 1/2 & 1/2 & 0 & 0 & 0 & 0 & 0 & 0 & 0 & 0 \\ -1 & 1 & 0 & 0 & 0 & 0 & 0 & 0 & 0 & 0 \\ 0 & 0 & 1/2 & 1/2 & 0 & 0 & 0 & 0 & 0 & 0 \\ 0 & 0 & -1 & 1 & 0 & 0 & 0 & 0 & 0 & 0 \\ 0 & 0 & 0 & 0 & 1 & 0 & 1 & 1 & 0 & 0 \\ 0 & 0 & 0 & 0 & 0 & 1 & 0 & 0 & 1 & 1 \end{pmatrix},$$

\mathbf{R}

whose inverse is:

$$\mathbf{M}_+^{-1} = \begin{pmatrix} 1 & -1/2 & 0 & 0 & 0 & 0 & 0 & 0 & 0 & 0 \\ 1 & 1/2 & 0 & 0 & 0 & 0 & 0 & 0 & 0 & 0 \\ 0 & 0 & 1 & -1/2 & 0 & 0 & 0 & 0 & 0 & 0 \\ 0 & 0 & 1 & 1/2 & 0 & 0 & 0 & 0 & 0 & 0 \\ 2/3 & 0 & 0 & 0 & 1/3 & 0 & -2/3 & -1/3 & 0 & 0 \\ 0 & 0 & 2/3 & 0 & 0 & 1/3 & 0 & 0 & -2/3 & -1/3 \\ -1/3 & 1/2 & 0 & 0 & 1/3 & 0 & 1/3 & -1/3 & 0 & 0 \\ -1/3 & -1/2 & 0 & 0 & 1/3 & 0 & 1/3 & 2/3 & 0 & 0 \\ 0 & 0 & -1/3 & 1/2 & 0 & 1/3 & 0 & 0 & 1/3 & -1/3 \\ 0 & 0 & -1/3 & -1/2 & 0 & 1/3 & 0 & 0 & 1/3 & 2/3 \end{pmatrix}.$$

We then eliminate the cyclic degrees of freedom $\tilde{\phi}_5$ and $\tilde{\phi}_6$. Given our solution choice for \mathbf{M} , the map between our and Ref. [9]'s notation is:

$$\begin{aligned} \tilde{\phi}_i &= \phi_j, \\ \tilde{\phi}_{i+1} &= \phi_{j\text{dc}}, \\ \phi_{x_i} &= \phi_{jx} - \frac{1}{2}\phi_{j\text{xdc}}, \text{ and} \\ \phi_{x_{i+1}} &= \phi_{j\text{xdc}}. \end{aligned}$$

Here, the index i corresponds either to the i th irrotational degree of freedom or i th external flux, while the index j corresponds to the j th $v\beta$ -rf SQUID, for which

$i = 1, 3$ and $j = 1, 2$, respectively.

Next, the inductive contribution to the potential, when taking $L := L_1 = L_2$ and $l := l_1 = l_2 = l_3 = l_4$, is found by first writing:

$$\mathbf{L} = \begin{pmatrix} L & -M & 0 & 0 & 0 & 0 \\ -M & L & 0 & 0 & 0 & 0 \\ 0 & 0 & l & 0 & 0 & 0 \\ 0 & 0 & 0 & l & 0 & 0 \\ 0 & 0 & 0 & 0 & l & 0 \\ 0 & 0 & 0 & 0 & 0 & l \end{pmatrix}.$$

Then, subsequently taking the inverse gives:

$$\mathbf{L}^{-1} = \begin{pmatrix} 1/L_\alpha & \mu/L_\alpha & 0 & 0 & 0 & 0 \\ \mu/L_\alpha & 1/L_\alpha & 0 & 0 & 0 & 0 \\ 0 & 0 & 1/l & 0 & 0 & 0 \\ 0 & 0 & 0 & 1/l & 0 & 0 \\ 0 & 0 & 0 & 0 & 1/l & 0 \\ 0 & 0 & 0 & 0 & 0 & 1/l \end{pmatrix},$$

where $L_\alpha = \alpha L$, $\alpha = 1 - \mu^2$, and $\mu = M/L$.

In Ref. [9]’s notation, the potential is

$$\begin{aligned} \mathcal{L}_V = & -E_{2+1} \cos \varphi_1 \cos \frac{\varphi_{1dc}}{2} + E_{2-1} \sin \varphi_1 \sin \frac{\varphi_{1dc}}{2} \\ & - E_{4+3} \cos \varphi_2 \cos \frac{\varphi_{2dc}}{2} + E_{4-3} \sin \varphi_2 \sin \frac{\varphi_{2dc}}{2} \\ & + \frac{1}{2l}(\phi_{1dc} - \phi_{1xdc})^2 + \frac{1}{2l}(\phi_{2dc} - \phi_{2xdc})^2 \\ & + \frac{1}{2L_\alpha}(\phi_1 - \phi_{1x})^2 + \frac{1}{2L_\alpha}(\phi_2 - \phi_{2x})^2 \\ & + \frac{\mu}{L_\alpha}(\phi_1 - \phi_{1x})(\phi_2 - \phi_{2x}). \end{aligned} \quad (17)$$

If we assume small coupling by keeping only linear terms in μ , then $L_\alpha^{-1} \rightarrow L^{-1}$, resulting in Eq. (17) simplifying to a sum of two $v\beta$ -rf SQUIDs potential contributions and a mutual inductance coupling $\mathcal{L}_{M.I.}$:

$$\mathcal{L}_V = \mathcal{L}_{v\beta\text{-rf } 1} + \mathcal{L}_{v\beta\text{-rf } 2} + \mathcal{L}_{M.I.} \quad (18)$$

The potential in Eq. (18) is shown in Fig. 3. We see four clear stable energy minima, that can be assigned to the computational memory states 00, 01, 10, and 11, respectively. Taking advantage of the metastable regions near each minimum, we can store information. By varying the values of M , ϕ_{ix} , and ϕ_{ixdc} , we can process that information—using the dynamics of the Euler-Lagrange equation of motion to implement various 2-bit logic gates.

V. CONCLUSION

We introduced a superconducting circuit formalism that permits exploring the classical informational processing properties of a proposed superconducting circuit through understanding the circuit’s energetics and subsequent dynamics. The techniques reproduce—with

much improved analytical efficiency—potentials used in experimentally investigating information-bearing degrees of freedom [4], as well as constructing a device that supports 2-bit computations. A sequel describes the information processing properties and performance in detail.

This is simply the first effort in a series on physically-realizable dynamical computing. In point of fact, the coupled $v\beta$ -rf SQUIDs shown in Fig. 2 also supports the information processing behavior exhibited by a Szilard engine [1, 30, 31]. Follow-on efforts explore the thermodynamic properties of these circuits, as well as implement 2-bit universal gates—e.g., NAND and NOR—and the universal reversible Fredkin gate using three coupled circuits.

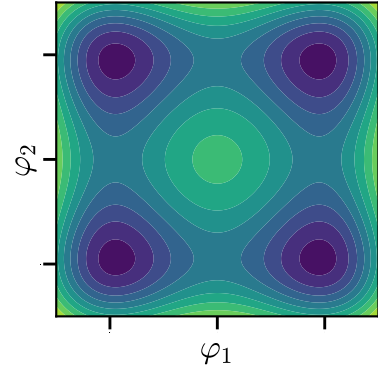


FIG. 3. Potential energy surface implied by Eq. (18) under “neutral” parameter values. We can store information by assigning each region surrounding a minimum to 00, 10, 01 and 11, respectively. Processing of information is accomplished by tuning the mutual inductance and external flux parameters to implement a control protocol.

VI. ACKNOWLEDGMENTS

The authors thank Scott Habermehl and Greg Wimsatt for helpful discussions, as well as the Telluride Science Research Center for its hospitality during visits and the participants of the Information Engines workshop there for their valuable feedback. J.P.C. acknowledges the kind hospitality of the Santa Fe Institute and California Institute of Technology. This material is based on work supported by, or in part by, the U.S. Army Research Laboratory and U.S. Army Research Office under Grant No. W911NF-21-1-0048.

* czpratt@ucdavis.edu

† kjay@ucdavis.edu

‡ chaos@ucdavis.edu

[1] A. B. Boyd and J. P. Crutchfield. Maxwell Demon Dynamics: Deterministic Chaos, the Szilard Map, and the Intelligence of Thermodynamic Systems. *Physical Review*

Letters, 116(19):190601, 2016.

[2] K. J. Ray, A. B. Boyd, G. W. Wimsatt, and J. P. Crutchfield. Non-Markovian momentum computing: Thermodynamically efficient and computation universal. *Physical Review Research*, 3(2), 2021.

- [3] R. Landauer. Irreversibility and heat generation in the computing process. *IBM Journal of Research and Development*, 5(3):183–191, 1961.
- [4] O.-P. Saira, M. H. Matheny, R. Katti, W. Fon, G. Wimsatt, J. P. Crutchfield, S. Han, and M. L. Roukes. Nonequilibrium thermodynamics of erasure with superconducting flux logic. *Physical Review Research*, 2(1), 2020.
- [5] K. J. Ray and J. P. Crutchfield. Gigahertz Sub-Landauer Momentum Computing. *Phys. Rev. Applied*, 19:014049, 2023.
- [6] T. Conte et al. Thermodynamic Computing, 2019.
- [7] A. B. Boyd, A. Patra, C. Jarzynski, and J. P. Crutchfield. Shortcuts to Thermodynamic Computing: The Cost of Fast and Faithful Information Processing. *Journal of Statistical Physics*, 187(2), 2022.
- [8] S. Han, J. Lapointe, and J. E. Lukens. Thermal activation in a two-dimensional potential. *Physical Review Letters*, 63(16):1712–1715, 1989.
- [9] S. Han, J. Lapointe, and J. E. Lukens. *Variable β rf SQUID*, volume 31, page 219–222. Springer Berlin Heidelberg, Berlin, Heidelberg, 1992.
- [10] R. Cantor. *Dc Squids: Design, Optimization and Practical Applications*, page 179–233. Springer Netherlands, Dordrecht, 1996.
- [11] T. P. Orlando et al. Superconducting persistent-current qubit. *Physical Review B*, 60(22):15398–15413, 1999.
- [12] M. Mück, B. Chesca, and Y. Zhang. *Radio Frequency SQUIDS and their Applications*, page 505–540. Springer Netherlands, Dordrecht, 2001.
- [13] M. H. Devoret. *Quantum Fluctuations in Electrical Circuits*. Elsevier Science, Les Houches, Session LXIII, 1995.
- [14] G. Burkard, R. H. Koch, and D. P. DiVincenzo. Multilevel quantum description of decoherence in superconducting qubits. *Physical Review B*, 69(6):064503, Feb 2004.
- [15] X. You, J. A. Sauls, and J. Koch. Circuit quantization in the presence of time-dependent external flux. *Physical Review B*, 99(17):174512, May 2019.
- [16] M. Mariantoni. The energy of an arbitrary electrical circuit, classical and quantum, 2021.
- [17] H. Goldstein, C. P. Poole, and J. L. Safko. *Classical Mechanics*. Addison-Wesley, San Francisco Munich, 3. ed. edition, 2008.
- [18] M. Xiang-Guo, W. Ji-Suo, Z. Yun, and F. Hong-Yi. Number-phase quantization and deriving energy-level gap of two lc circuits with mutual-inductance. *Chinese Physics Letters*, 25(4):1205–1208, 2008.
- [19] M. Xiang-Guo, W. Ji-Suo, and L. Bao-Long. Cooper-pair number-phase quantization for inductance coupling circuit including josephson junctions. *Chinese Physics Letters*, 25(4):1419–1422, 2008.
- [20] S. P. Chitta, T. Zhao, Z. Huang, I. Mondragon-Shem, and J. Koch. Computer-aided quantization and numerical analysis of superconducting circuits. *New Journal of Physics*, Sep 2022.
- [21] J. Ulrich and F. Hassler. Dual approach to circuit quantization using loop charges. *Physical Review B*, 94(9):094505, Sep 2016.
- [22] R.-P. Riwar and D. P. DiVincenzo. Circuit quantization with time-dependent magnetic fields for realistic geometries. *npj Quantum Information*, 8(1):36, Mar 2022.
- [23] W. C. Stewart. Current-voltage characteristics of josephson junctions. *Applied Physics Letters*, 1968.
- [24] D. E. McCumber. Effect of ac Impedance on dc Voltage-Current Characteristics of Superconductor Weak-Link Junctions. *Journal of Applied Physics*, 39(7):3113–3118, 1968.
- [25] S. Han, J. Lapointe, and J. E. Lukens. Effect of a two-dimensional potential on the rate of thermally induced escape over the potential barrier. *Physical Review B*, 46(10):6338–6345, 1992.
- [26] B. Yurke and J. S. Denker. Quantum network theory. *Physical Review A*, 29(3), 1984.
- [27] A. van den Brink, A. J. Berkley, and M. Yalowsky. Mediated tunable coupling of flux qubits. *New Journal of Physics*, 7:230–230, Nov 2005.
- [28] R. Harris et al. Sign- and magnitude-tunable coupler for superconducting flux qubits. *Physical Review Letters*, 98(17):177001, Apr 2007.
- [29] I. Ozfidan et al. Demonstration of a nonstoquastic hamiltonian in coupled superconducting flux qubits. *Physical Review Applied*, 13:034037, Mar 2020.
- [30] L. Szilard. Über die ausdehnung der phänomenologischen thermodynamik auf die schwankungserscheinungen. *Zeitschrift für Physik*, 32(1):753–788, 1925.
- [31] L. Szilard. On the decrease of entropy in a thermodynamic system by the intervention of intelligent beings. *Behavioral Science*, 1964.